Long-range collectivity in small collision systems with two- and four-particle correlations at STAR

doi: 10.1016/j.nuclphysa.2018.09.072

Available online at www.sciencedirect.com

ScienceDirect

Nuclear Physics A 982 (2019) 475–478

www.elsevier.com/locate/nuclphysa

Long-range collectivity in small collision systems with two- and four-particle correlations at STAR

Shengli Huang (for the STAR Collaboration)

Department of Chemistry, Stony Brook University, Stony Brook, NY, 11794-3400, USA

Abstract

New STAR measurements of two- and four-particle ($c_2\{4\}$) azimuthal angle correlations are reported for p+Au collisions at 200 GeV and d+Au collisions from 19.6 to 200 GeV. A negative $c_2\{4\}$, consistent with collective anisotropic flow, is observed in high multiplicity d+Au events at 62.4 and 200 GeV where the statistical significance of the data allows an analysis. A template fitting method, employed to subtract non-flow contributions to the two-particle correlations, allows the extraction of the anisotropy coefficients (v_2) for these systems at their respective energies. The v_2 results for different energies show a common dependence on the charged particle multiplicity density ($\langle dN_{ch}/d\eta \rangle$), which provide important insight on the nature of collective behavior in small collision systems.

Keywords: two- and four-particle azimuthal angular correlations, ridge, anisotropic flow, cumulant

1. Introduction

Recent measurements at both the LHC [1–5] and RHIC [6–9] have discovered and confirmed the presence of long-range two-particle angular correlations (the so-called 'ridge') in high-multiplicity p+p and $p/d/^3$He+A collisions. The magnitude of the associated azimuthal anisotropy can be obtained from a Fourier expansion of the azimuthal angle (ϕ) distribution of the emitted hadrons.

Several models, which include initial-state gluon saturation [10–12] and hydrodynamic flow [13–17], have been employed to explain the observed anisotropies. However, a consensus on the theoretical interpretation of the long-range correlations has not been reached.

In this work, we utilize $\langle dN_{ch}/d\eta \rangle$ and beam-energy-dependent measurements for p+Au and d+Au collisions to gain further insights on the ridge physics. The observed anisotropy in these systems provide new information to address the physics origin of 'ridge', as well as to expose possible limitations to the fluid dynamical description of the matter created in these collisions.

2. Analysis methods

In this analysis, event classes are defined as a percentile of the total charge measured by the beam-beam counter (BBC) spanning the pseudo-rapidity range -5.0 < η < -3.3 on the Au-going side. The $\langle dN_{ch}/d\eta \rangle$ for each event class is then measured in $|\eta| < 0.9$ for the transverse momentum range 0.2 GeV/c < p_T < 3.0 GeV/c, in the STAR Time Projection Chamber (TPC), which covers 2π in azimuth and $|\eta| < 1.0$. To remove

https://doi.org/10.1016/j.nuclphysa.2018.09.072
0375-9474/

pileup events, charged tracks were required to match a hit measured by the Time of Flight (TOF) detector and had a tight cut of distance of closet approach (DCA < 3.0 cm) to the primary vertex. A comparison of the measurements for different beam luminosities was used to estimate the systematic uncertainty for possible residual pileup. Candidate particle pairs from these event samples were used to construct two-particle $Y(\Delta\phi)$ correlators for further analysis.

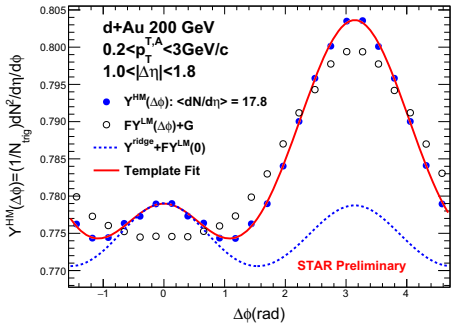

Fig. 1. Two-particle azimuthal angular correlations ($Y(\Delta\phi)$) for 0-10% d+Au collisions at $\sqrt{s_{NN}}$ = 200 GeV. A template fitting procedure is employed to extracted the flow parameters using the LM event to estimate the non-flow contributions.

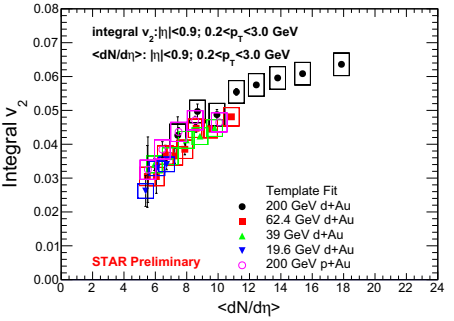

Fig. 2. The integral v_2 from template fitting as a function of $\langle dN_{ch}/d\eta\rangle$ in d+Au collisions. Results are shown for several beam energies as indicated.

A representative two-particle $Y(\Delta\phi)$ distribution for high multiplicity (HM) events (top 10% of total BBC charge) is shown as a function of $\Delta\phi$ in Fig. 1. The trigger- and the associated-particles are measured in the ranges 0.2 GeV/c< p_T < 3.0 GeV/c and $|\eta| < 0.9$. A clear ridge peak is observed for this event class. To separate the ridge from the non-flow angular correlations which dominate low multiplicity (LM) events, a template fitting procedure was applied to the measured $Y(\Delta\phi)$ distributions [18] as illustrated in Fig. 1. The method assumes that the HM $Y(\Delta\phi)$ distributions are a superposition of a scaled LM $Y(\Delta\phi)$ distribution and a constant modulated by $\sum_{n=2}^{4} V_{n,n}\cos(n\Delta\phi)$ as:

$$Y(\Delta\phi)^{templ} = FY(\Delta\phi)^{LM} + Y(\Delta\phi)^{ridge}, \tag{1}$$

where

$$Y(\Delta\phi)^{ridge} = G\left(1 + 2\sum_{n=2}^{4} V_{n,n}\cos\left(n\Delta\phi\right)\right), \tag{2}$$

with free parameters F and $V_{n,n}$. The coefficient G, which represents the magnitude of the combinatoric component of $Y(\Delta\phi)^{ridge}$, is fixed by requiring that $\int_0^\pi d\Delta\phi\ Y^{\rm templ} = \int_0^\pi d\Delta\phi\ Y^{\rm HM}$. The LM distribution was obtained from the peripheral (90-100%) event class. Since the trigger- and the associated particles are measured in the same p_T range, the integral $v_2 = \sqrt{V_{2,2}}$.

The four-particle cumulant method was also used to study the long-range correlations. The operational details of the cumulant method can be found in Refs. [19, 20]. In brief, the two- and four-particle azimuthal correlators are constructed by averaging over all tracks in a given event, then over all events as [19, 21]:

$$\langle\langle 2m\rangle\rangle \quad = \quad \langle\langle e^{in\sum_{j=1}^{m}(\phi_{2j-1}-\phi_{2j})}\rangle\rangle. \tag{3}$$

The corresponding four-particle cumulants are obtained as:

$$c_n\{4\} \quad = \quad \langle\langle 4\rangle\rangle - 2\langle\langle 2\rangle\rangle^2 \tag{4}$$

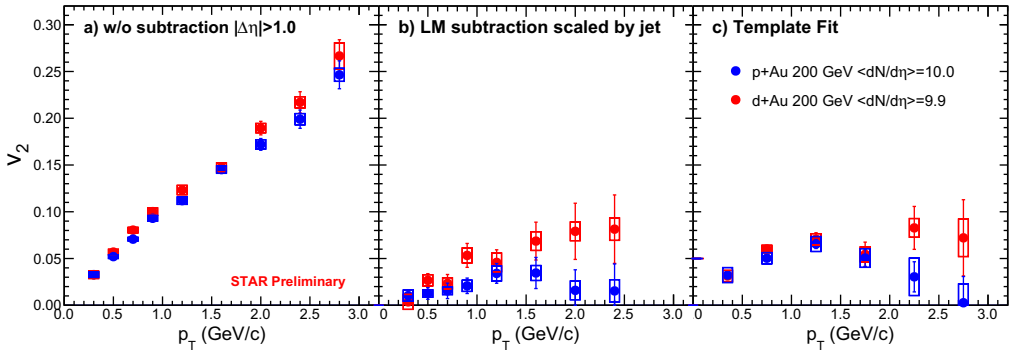

Fig. 3. Comparison of v_2 vs. p_T in p+Au and d+Au collisions at $\sqrt{s_{NN}}$ = 200 GeVfor event classes leading to $\langle dN_{ch}/d\eta \rangle \sim 10$. Panels (a), (b) and (c) show comparisons of the v_2 values for the unsubtracted, non-flow subtraction with method (i) and non-flow-subtraction with method (ii) respectively (see text).

3. Results

The template fitting method was employed to measure the integral v_2 values as a function of $\langle N_{ch} \rangle$ in d+Au collisions from 19.6 to 200 GeV and p+Au at 200 GeV. The values for both v_2 and $\langle dN_{ch}/d\eta \rangle$ were evaluated for 0.2 GeV/c$< p_T <$ 3.0 GeV/c and $|\eta| < 0.9$ for each data set. Fig. 2 shows similar magnitudes and trends for v_2 values extracted at similar $\langle dN_{ch}/d\eta \rangle$ irrespective of beam energy and system. This observation is consistent with the expected trend for the dominance of final-state viscous attenuation at low $\langle dN_{ch}/d\eta \rangle$ [22]. Note that the eccentricity difference of ~ 2, obtained for p+Au and d+Au with the nucleon Glauber model [23] , is substantially less than the corresponding difference obtained from initial-state geometric models which take account of the internal structure of the nucleons [22, 24]. In the latter models, the beam energy dependence of the initial-state eccentricity for d+Au collisions is rather weak as well.

To further compare v_2 in p+Au and d+Au collisions, event classes were selected so as to give the same $\langle dN_{ch}/d\eta \rangle \sim 10$ for both systems. In addition, two different methods of non-flow subtraction were employed; (i) LM subtraction scaled by near-side jet yield [25–27]; and (ii)template fitting. The resulting v_2 values are shown as a function of p_T in Fig. 3. The subtracted v_2 shown on panels (b) and (c) are smaller than the un-subtracted v_2 shown in panel (a), it indicates there are substantial non-flow contributions for $\langle dN_{ch}/d\eta \rangle \sim 10$. However, they do not indicate a sizable difference in the magnitudes for the d+Au and p+Au results. This observation is in line with the small system-dependent eccentricity difference alluded to earlier.

Results from four-particle angular correlation measurements in d+Au collisions, are shown in the Fig. 4. The efficiency corrected multiplicity and $c_2\{4\}$ were similarly measured using charged hadrons within $|\eta| <$0.9 in the TPC, and for 0.2 GeV/c $< p_T <$ 3.0 GeV/c. For high multiplicity events, a negative $c_2\{4\}$ is observed for d+Au collisions at 62.4 and 200 GeV, albeit with sizable statistical uncertainties. The negative $c_2\{4\}$ values are consistent with the expectation for anisotropic flow in the most central d+Au collisions at 62.4 and 200 GeV.

4. Summary

In this proceeding, we have presented two- and four-particle azimuthal angle correlation measurements for p+Au and d+Au collisions at different collision energies, as a function of p_T and mean $\langle dN_{ch}/d\eta \rangle$. The integral v_2 (0.2 GeV/c $< p_T <$ 3.0 GeV/c) extracted with a template fitting procedure to account for non-flow effects, shows a common $\langle dN_{ch}/d\eta \rangle$ dependent trend, irrespective of colliding species and the beam

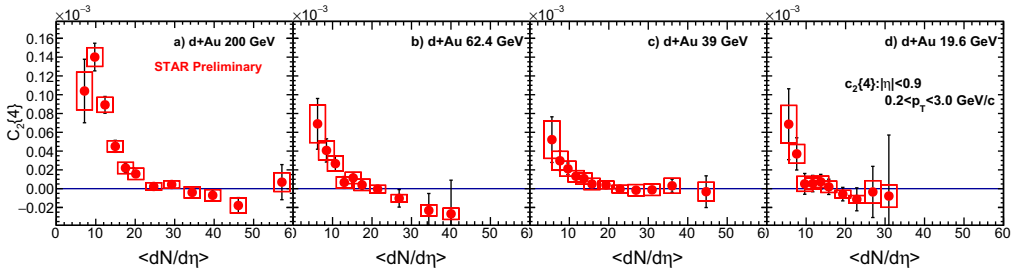

Fig. 4. $c_2\{4\}$ vs. $\langle dN_{ch}/d\eta\rangle$ for d+Au collisions at several beam energies as indicated. Note the negative $c_2\{4\}$ values for large $\langle dN_{ch}/d\eta\rangle$ in collisions at 62.4 and 200 GeV.

energy. For event classes with the same $\langle dN_{ch}/d\eta\rangle$, a similar $v_2(p_T)$ pattern is observed for p+Au and d+Au collisions at 200 GeV after non-flow subtraction. In high multiplicity events, a negative $c_2\{4\}$ is observed in d+Au collisions at 200 and 62.4 GeV respectively. The combined results from these measurements indicate that the anisotropy of particle emissions in high multiplicity p+Au and d+Au collisions is strongly influenced by final-state anisotropic flow. While other contributions such as from initial state correlation [12] still can not be ruled out.

5. Acknowledgments

This research is supported by the US Department of Energy under contract DE-FG02-87ER40331.A008.

References

[1] S. Chatrchyan, et al., Phys.Lett. B718 (2013) 795–814.
[2] G. Aad, et al., Phys. Rev. Lett. 110 (2013) 182302.
[3] B. Abelev, et al., Phys.Lett. B719 (2013) 29–41.
[4] G. Aad, et al., Phys.Lett. B725 (2013) 60–78.
[5] S. Chatrchyan, et al., Phys.Lett. B724 (2013) 213–240.
[6] L. Adamczyk, et al., Phys. Lett. B 747 (2015) 265.
[7] A. Adare, et al., Phys. Rev. Lett. 111 (2013) 212301.
[8] A. Adare, et al., Phys. Rev. Lett. 114 (2015) 192301.
[9] A. Adare, et al., Phys. Rev. Lett. 115 (2015) 142301.
[10] K. Dusling, R. Venugopalan, Phys.Rev.Lett. 108 (2012) 262001.
[11] K. Dusling, R. Venugopalan, Phys.Rev. D87 (2013) 094034. arXiv:1302.7018.
[12] M. Mace, et al., Phys.Rev.Lett. 121 (2018) 052301.
[13] E. Avsar, C. Flensburg, Y. Hatta, J.-Y. Ollitrault, T. Ueda, Phys.Lett. B702 (2011) 394–397.
[14] K. Werner, I. Karpenko, T. Pierog, Phys.Rev.Lett. 106 (2011) 122004.
[15] P. Bozek, Phys.Rev. C85 (2012) 014911.
[16] E. Shuryak, I. Zahed, Phys.Rev. C88 (2013) 044915.
[17] G.-Y. Qin, B. Muller, Phys.Rev. C89 (2014) 044902.
[18] G. Aad, et al., Phys. Rev. Lett. 116 (2016) 172301.
[19] A. Bilandzic, R. Snellings, S. Voloshin, Phys. Rev. C83 (2011) 044913. arXiv:1010.0233.
[20] A. Bilandzic, C. H. Christensen, K. Gulbrandsen, A. Hansen, Y. Zhou, Phys. Rev. C89 (6) (2014) 064904. arXiv:1312.3572.
[21] N. Borghini, P. M. Dinh, J.-Y. Ollitrault, Phys. Rev. C64 (2001) 054901. arXiv:nucl-th/0105040.
[22] P. Liu, R. A. LaceyarXiv:1804.04618.
[23] J. L. Nagle, A. Adare, S. Beckman, T. Koblesky, J. O. Koop, D. McGlinchey, P. Romatschke, J. Carlson, J. E. Lynn, M. McCumber, Exploiting Intrinsic Triangular Geometry in Relativistic ^{3}He+Au Collisions to Disentangle Medium Properties, Phys. Rev. Lett. 113 (11) (2014) 112301. doi:10.1103/PhysRevLett.113.112301.
[24] K. Dusling, et al.arXiv:1509.07939.
[25] L. Adamczyk, et al., Phys. Lett. B 743 (2015) 333.
[26] G. Aad, et al., Phys. Rev. C90 044906.
[27] V. Khachatryan, et al., Phys. Lett. B 765 (2017) 193 – 220.